Chapter 6

In Vivo Monitoring of Nucleophagy in *Caenorhabditis elegans*

Georgios Konstantinidis and Nektarios Tavernarakis

Abstract

The autophagy-lysosomal pathway enables the controlled degradation of cellular contents. Nucleophagy is the selective autophagic recycling of nuclear components upon delivery to the lysosome. Although methods to monitor and quantify autophagy as well as selective types of autophagy have been developed and implemented in cells and in vivo, methods monitoring nucleophagy remain scarce. Here, we describe a procedure to monitor the autophagic engagement of an endogenous nuclear envelope component, i.e., ANC-1, the nematode homologue of the mammalian Nesprins in vivo, utilizing super-resolution microscopy.

Key words ANC-1, Autophagy, *Caenorhabditis elegans*, LGG-1, Nesprin, Nucleophagy, Nucleus, Super-resolution microscopy

1 Introduction

The linker of nucleoskeleton and cytoskeleton (LINC) complexes comprise a conserved network of proteins supporting nucleus and nuclear envelope architecture [1]. They mediate fundamental cellular functions, including nuclear positioning, nucleoskeleton-cytoskeleton communication, mechanotransduction, homolog pairing in meiosis, DNA damage repair, and others [2, 3]. LINC complexes span the nuclear envelope and consist of Sad1 and UNC-84 (SUN) proteins at the inner nuclear membrane and Klarsicht, ANC-1, and Syne homology (KASH) proteins in the outer nuclear membrane [1]. Defects in nuclear positioning and mutations in LINC components are associated with a wide variety of human diseases [2, 3].

Previous studies in *Caenorhabditis elegans* (*C. elegans*) have contributed to our current understanding regarding nuclear positioning during development [4–7]. ANC-1 (orthologous to mammalian SYNE1/Nesprin-1 and SYNE2/Nesprin-2), is one of the

Ioannis P. Nezis (ed.), *Selective Autophagy: Methods and Protocols*, Methods in Molecular Biology, vol. 2845,
https://doi.org/10.1007/978-1-0716-4067-8_6,

four KASH proteins in *C. elegans*, which are localized to the outer nuclear membrane where they connect the nucleus to the cytoskeleton [8–10]. ANC-1 mediates nuclear anchorage through its interaction with the SUN protein UNC-84 at the inner nuclear membrane and actin cytoskeleton in the cytoplasm [10]. In addition, ANC-1 localizes to the endoplasmic reticulum (ER) membrane to position nuclei as well as other organelles in place [11]. Nesprin mutations perturbing Nesprin/Emerin/Lamin interactions can cause uncoupling of the nucleoskeleton from the cytoskeleton. Such mutations lead to two distinct human neurological or myopathic disease phenotypes, a feature similar to that found in laminopathies. Specifically, Nesprin dysregulated levels or Nesprin mutations are associated with spinocerebellar ataxias [12–16], autism [17, 18], bipolar disorders [19, 20], major depression [20], Emery-Dreifuss Muscular Dystrophy [21, 22], dilated cardiomyopathy [23], arthrogryposis multiplex congenita [24], cancer [25–32], and hearing loss [33].

The dynamics of the nucleus and the nuclear envelope confer plasticity and support nuclear functions. Quality control mechanisms ensure the maintenance of nuclear architecture and integrity. For example, the endosomal sorting complex required for transport (ESCRT) machinery functions to surveil nuclear pore complex (NPC) assembly, remodel the nuclear envelope in response to mechanical cues or rupture, and accomplish sealing of the postmitotic nuclear envelope [34]. Nucleophagy serves as the selective subtype of autophagy targeting nuclear components for degradation in lysosomes [35]. Autophagic engagement of nuclear content, such as DNA fragments, histones, and lamins, has been shown in different physiological or pathological settings in cells as well as in vivo, using predominantly fluorescence microscopy [36–46]. On the one hand, immuno- or direct staining enables the identification of endogenous cargo into autophagosomes in fixed samples by colocalization with autophagic proteins such as LC3, since a mammalian receptor of nucleophagy has not been identified yet. On the other hand, a fluorescently tagged protein of interest can be monitored in living cells by exogenous expression concomitantly with an autophagy reporter protein. Here, we describe a procedure to monitor nucleophagy by capturing the autophagic engagement of an endogenous nuclear component in vivo, using super-resolution microscopy.

Autophagy is a dynamic process, and visualizing subtle or rare autophagosome formation events can be challenging. Furthermore, autophagic engagement of nuclear components is rarely captured, especially under physiological conditions. In order to increase the probability of monitoring such events, two approaches are followed. First, in order to induce increased autophagic or selective nucleophagic activity, *daf-2(RNAi)* (Fig. 1) or nuclear insults such as DNA damage (etoposide or mitomycin C treatment)

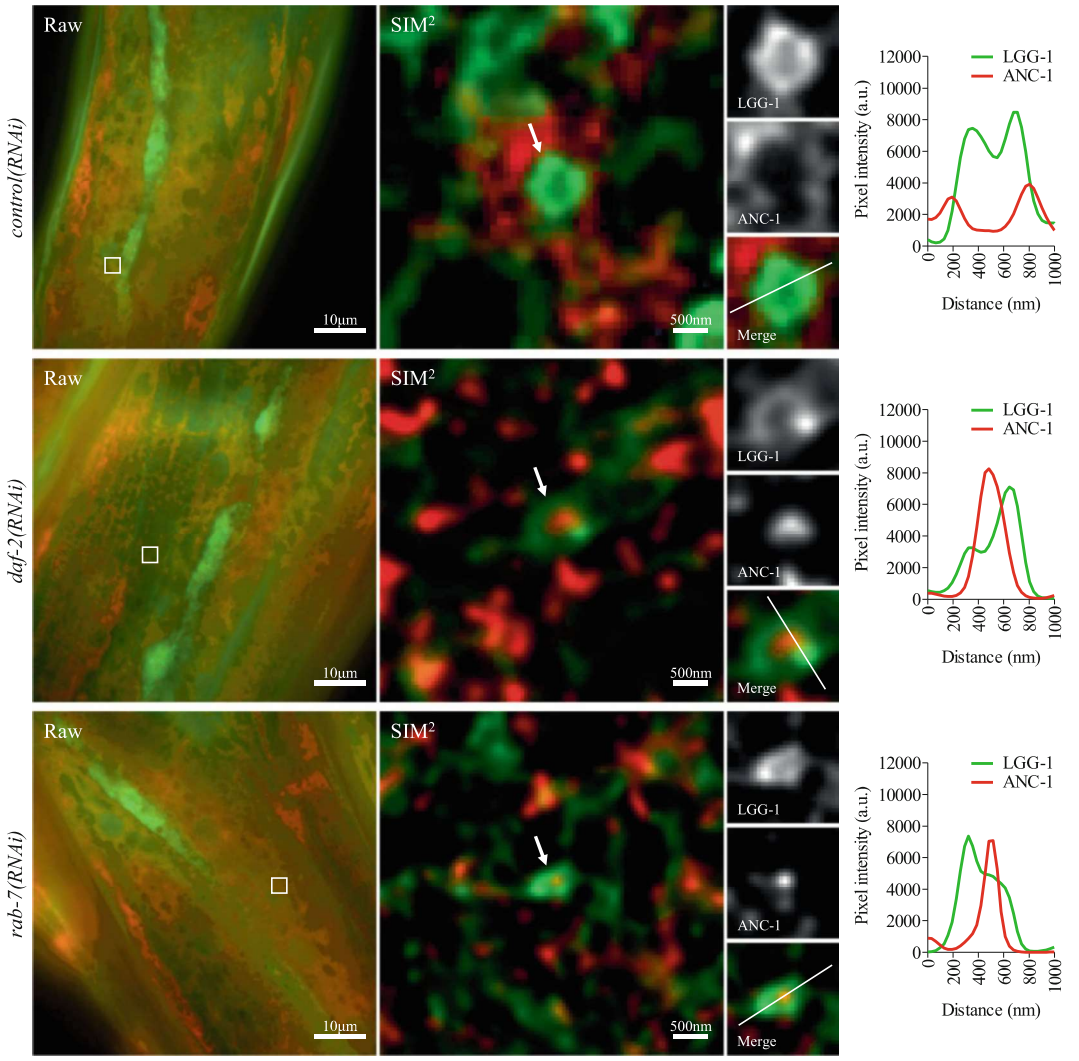

Fig. 1 Monitoring nucleophagy upon genetic manipulation of autophagy, in vivo. The first of the 15 lattice SIM phase images is presented as a raw image with merged 488 nm (GFP::LGG-1) and 561 nm (mKate2::ANC-1) channels. SIM^2 images show areas of SIM processing corresponding to the boxes in raw images. White arrows point to autophagosomes, which are presented in both separate channels (LGG-1 and ANC-1) and merged images. Pixel intensity measurements correspond to the respective white line of 1 μm length. Note ANC-1 engulfment into LGG-1 positive structures upon autophagy induction [*daf-2(RNAi)*] or inhibition of autophagosome-lysosome fusion [*rab-7(RNAi)*]

(Fig. 2) are applied, respectively. The latter could serve as a specific nucleophagy induction condition. Second, by blocking the autophagosome-lysosome fusion step, it is possible to accumulate autophagic structures in order to quantify the autophagosome formation events as well as monitor their contents [47]. Lysosomotropic agents, such as chloroquine, or *daf-2(RNAi)* (Fig. 1) serve as autophagic flux inhibitors. The second perturbation serves as a

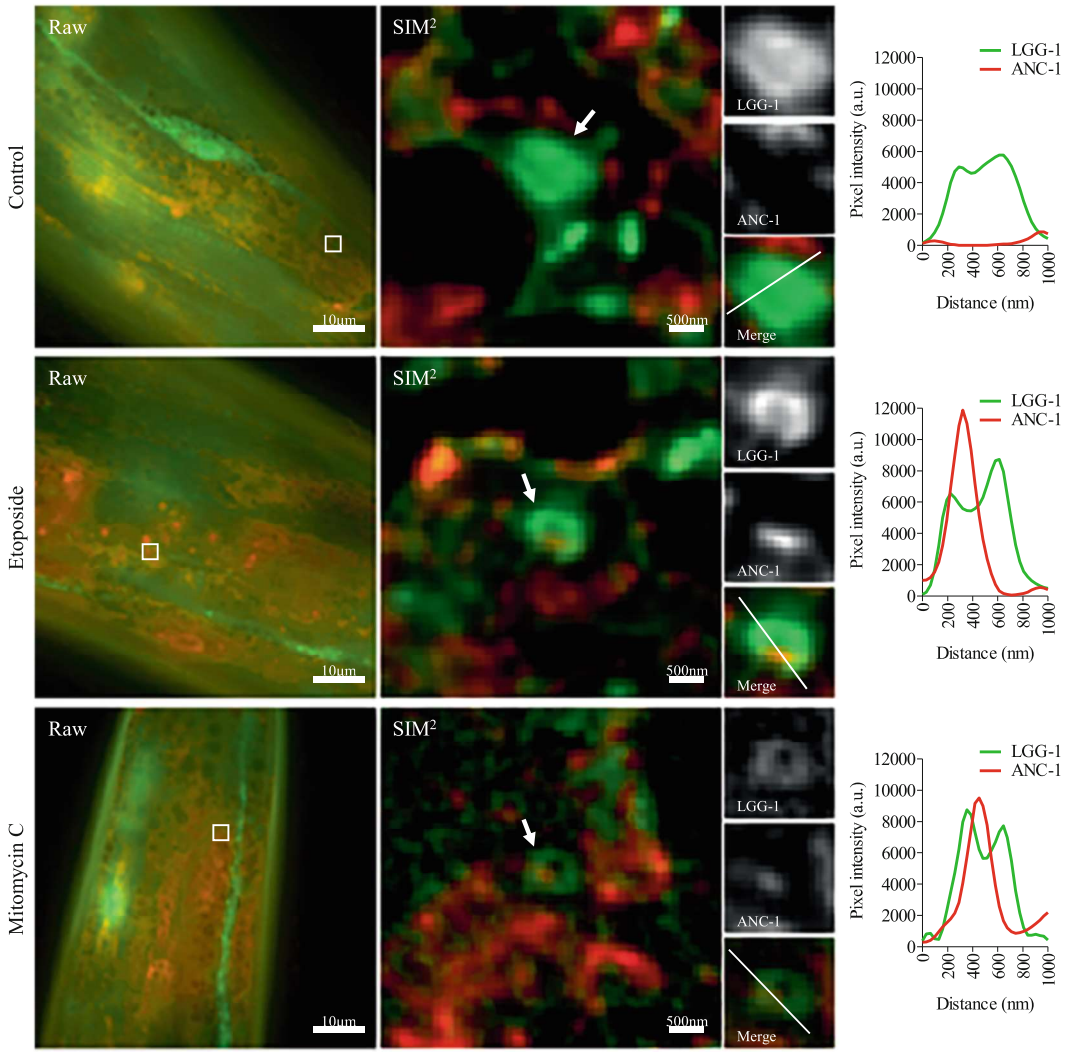

Fig. 2 Monitoring nucleophagy upon DNA damage, in vivo. The first of the 15 lattice SIM phase images is presented as a raw image with merged 488 nm (GFP::LGG-1) and 561 nm (mKate2::ANC-1) channels. SIM^2 images show areas of SIM processing corresponding to the boxes in raw images. White arrows point to autophagosomes, which are presented in both separate channels (LGG-1 and ANC-1) and merged images. Pixel intensity measurements correspond to the respective white line of 1 μm length. Note ANC-1 engulfment into LGG-1 positive structures upon DNA damaging conditions

general approach to accumulate autophagic structures. Autophagy/nucleophagy induction and autophagic flux inhibition can be combined in order to increase the levels of nucleophagic events monitored.

Given that the nuclear envelope and ER form a contiguous network, ER-phagy and nucleophagy may occur concurrently [48, 49]. For example, the yeast protein Yep1, the ortholog of human receptor accessory proteins (REEP1-4), is essential for the

autophagosomal enclosure of cargo membrane structures derived from both the ER and nuclear envelope [50]. Yep1 function is specific to these two types of selective autophagy but not to bulk autophagy. Therefore, the above approach enables the identification of autophagic cargo composition and the monitoring of nuclear/ER membrane-specific capture. The application described here can shed light on numerous other unexplored segments of nucleophagy in vivo, such as nucleophagic signaling, regulation, and molecular mechanisms, in health and disease.

2 Materials

Prepare all solutions using analytical grade reagents.

2.1 Caenorhabditis elegans *Strains*

All experiments are carried out using hermaphrodite worms. The strain DA2123, *adIs2122* [*lgg-1p::GFP::lgg-1+rol-6(su1006)*], is provided by the Caenorhabditis Genetics Center (https://cgc.umn.edu/), which is funded by NIH Office of Research Infrastructure Programs (P40 OD010440). The strain UD626: *yc72* [*mKate2::anc-1b*] is a kind gift from Daniel A. Starr. The strain IR2969: *yc72* [*mKate2::anc-1b*]; *adIs2122* [*lgg-1p::GFP::lgg-1+rol-6(su1006)*] was generated in a previous study [46].

2.2 *Bacteria Strains*

OP50 uracil auxotroph *Escherichia coli*: Streak OP50 bacteria on a 100 mm plate from a glycerol stab and grow overnight at 37 °C. Inoculate a single OP50 colony into 50 mL of sterile liquid LB medium. Incubate for 5 h in a shaking incubator at 37 °C. Seed 200 μL of the OP50 culture in the middle of freshly prepared NGM plates, and let bacteria grow overnight at room temperature. Make use of the plates within the next 2 days. Store liquid OP50 culture at 4 °C. HT115 (DE3) *Escherichia coli* are used for *RNAi* experiments.

2.3 *Stock Solutions*

1. 1 M $CaCl_2$ (100 mL): Dissolve 14.7 g $CaCl_2$ in 100 mL ultrapure water and autoclave. Store at room temperature.
2. 1 M $MgSO_4$ (100 mL): Dissolve 24.65 g $MgSO_4$ in 100 mL ultrapure water and autoclave. Store at 4 °C.
3. 5 mg/mL cholesterol (200 mL): Dissolve 1 g cholesterol in 200 mL ethanol. Do not autoclave. Store at 4 °C.
4. 10 mg/mL nystatin (200 mL): Dissolve 2 g nystatin in 200 mL 70% ethanol. Do not autoclave. Mix thoroughly before use. Store at 4 °C.
5. 1 M KPO_4 (100 mL): Dissolve 102.2 g KH_2PO_4 and 57.06 g K_2HPO_4 in 100 mL ultrapure water, adjust pH to 6.0, and autoclave. Store at 4 °C.

6. 5 N NaOH (50 mL): Dissolve 10 g NaOH in 50 mL ultrapure water. Store at room temperature.
7. 2% NaN_3 (50 mL): Dissolve 1 g NaN_3 in 50 mL M9 solution. Store at room temperature.
8. 100 mg/mL ampicillin (10 mL): Dissolve 1 g ampicillin in 10 mL ultrapure water. Aliquot and store at −20 °C.
9. 5 mg/mL tetracycline (10 mL): Dissolve 50 mg tetracycline in 10 mL ethanol. Aliquot and store at −20 °C.
10. IPTG master stock (1 M): Dissolve 2.38 g isopropyl β- d-1-thiogalactopyranoside in 10 mL ultrapure water. Aliquot and store at −20 °C.
11. IPTG stock (20 mM): Mix 20 μL IPTG (1 M) with 980 μL ultrapure water. Aliquot and store at −20 °C.
12. Etoposide (50 mM): Dissolve 25 mg etoposide in 850 μL DMSO. Aliquot and store at −20 °C.
13. Mitomycin C (1 mg/mL): Dissolve 2 mg mitomycin C in 2 mL ultrapure water. Aliquot and store at −20 °C.

2.4 Working Solutions

1. M9 minimal medium solution (1 L): Dissolve 3 g KH_2PO_4, 6 g Na_2HPO_4 and 5 g NaCl in 800 mL ultrapure water and sterilize by autoclaving. Cool down at room temperature to approximately 50–55 °C. Add 1 mL $MgSO_4$ (1 M) post sterilization. Top up to 1 L with sterile ultrapure water. Store at room temperature.
2. Bleaching solution (10 mL): Mix 7 mL ultrapure water, 2 mL common NaOCl (5%), and 1 mL NaOH (5 N). Store at room temperature.
3. 0.1% NaN_3 (1 mL): Mix 50 μL NaN_3 (2%) with 950 μL ultrapure water. Store at room temperature.

2.5 Growth Media

1. Nematode growth medium (NGM) (1 L): Dissolve 3 g NaCl, 2.5 g bactopeptone, 0.2 g streptomycin, and 17 g agar in 800 mL ultrapure water and sterilize by autoclaving. Cool down at room temperature to approximately 50–55 °C. Add 1 mL $CaCl_2$ (1 M), 1 mL $MgSO_4$ (1 M), 1 mL cholesterol (5 mg/mL), 1 mL nystatin (10 mg/mL), and 25 mL KPO_4 (1 M). Top up to 1 L with sterile ultrapure water. Dispense 7 mL to 60 mm dishes and let solidify at room temperature. Store at 4 °C the next day.
2. Luria–Bertani (LB) liquid medium (1 L): Dissolve 10 g NaCl, 10 g tryptone, and 5 g yeast extract in 1 L ultrapure water. Stir until the mixture is completely dissolved. Sterilize by autoclaving.

3. Luria–Bertani (LB) solid medium (1 L): Dissolve 10 g NaCl, 10 g tryptone, 5 g yeast extract, and 15 g agar in 1 L ultrapure water. The powder will not be dissolved completely; the agar will be dissolved after autoclaving. Sterilize by autoclaving and cool down at room temperature to approximately 50–55 °C. Dispense 17 mL medium to 100 mm petri plates and let solidify at room temperature. Store at 4 °C the next day.
4. *RNAi* growth media: Follow the procedure for NGM without the addition of streptomycin. Add 500 μL ampicillin (100 mg/mL) post sterilization. Add 60 μL tetracycline (5 mg/mL) right before use and spread evenly. Let plates dry for 1 h.

3 Methods

3.1 Maintenance

The strain IR2969 is maintained well-fed for at least three generations at 20 °C. Do not let the worms undergo starvation to any degree.

3.2 Bleaching

Harvest gravid adult worms from one 60 mm plate with 1.6 mL of M9 solution. Transfer the solution to a 1.5 mL tube. Spin down and discard the M9 solution. Wash with 1 mL of M9 solution. Spin down and discard the M9 solution. Add 500 μL of bleaching solution. Rotate at room temperature for 2–3 min or until worms are dissolved and only eggs are left. Centrifuge for 30 s at maximum speed. Discard the bleaching solution. Wash with 1 mL of M9 solution, centrifuge for 30 s at maximum speed, and discard the M9 solution. Repeat the wash. In the last wash, keep approximately 100 μL of M9 solution. Resuspend the eggs and place them on fresh OB50 60 mm plates.

3.3 RNAi Silencing

1. Day 1: Streak *control(RNAi)*, *rab-7(RNAi)*, and *daf-2 (RNAi)* HT115 onto LB/ampicillin/tetracycline plates. Grow overnight at 37 °C.
2. Day 2: Grow overnight starter cultures from single colonies in 5 mL LB/ampicillin/tetracycline at 37 °C (shaking).
3. Day 3: Mix 70 μL of the overnight culture with 1 mL LB/ampicillin and incubate for 4 h at 37 °C (shaking). Mix 900 μL of the culture with 100 μL IPTG (20 mM) and seed 200 μL from each strain in the middle of respective *RNAi* plates. Let bacteria grow overnight at room temperature. Make use of them the next day (*see* **Note 1**).

3.4 Chemical Treatments

1. DMSO control: Mix 7 μL of DMSO with 133 μL of ultrapure water.

2. 50 μM etoposide: Mix 7 μL of etoposide (50 mM) with 133 μL of ultrapure water.
3. 20 μg/mL mitomycin C: Use 140 μL of mitomycin C (1 mg/mL).

   Inactivate OP50 loan on 60 mm NGM plates using ultraviolet crosslinking. Apply each of the above mixtures to one UV-inactivated OP50 plate for each condition and spread evenly. Let the plates dry for 1 h at room temperature and place eggs after bleaching (*see* **Note 2**).

3.5 Sample Preparation for Imaging

To prepare 2% agarose pads, add 0.5 g of agarose into 25 mL of M9 solution. Heat in the microwave (do not boil) until the agarose is completely dissolved. While the agarose is still hot, add a droplet of approximately 1 cm in diameter to the middle of a microscope glass slide using a 1 mL pipette (*see* **Note 3**). Immediately place another glass slide vertically on top to spread the agarose evenly and flatten it to a larger area. Let the agarose solidify for 1 min, then carefully remove the second glass slide without disturbing the agarose layer. Keep the agarose pad in the center of the glass slide. Store at room temperature (*see* **Note 4**). Add 3 μL of NaN_3 to the center of the agarose pad slide (*see* **Note 5**). Transfer worms from the plate to the agarose pad using an eyelash hair pick. Cover with an 18 mM × 18 mM coverslip. Add more NaN_3 at the edges of the coverslip until all coverslip area is covered to keep the worms wet. Seal and fix by applying nail polish at the edge of the coverslip. Proceed to imaging.

3.6 Super Resolution Structured Illumination Microscopy (SIM) and Analysis

Acquire fluorescent images using a ZEISS Elyra 7 microscope equipped with a Plan apochromat 63×/1.4 oil DIC M27 objective. Record mKate2 fluorescence using a 561 nm track with 30% intensity and 50 ms exposure. Record GFP fluorescence using a 488 nm track with 20% intensity and 50 ms exposure. Use the Carl Zeiss Zen 3.0 SR FP2 software for acquisition and SIM^2 analysis with default settings in weak live mode. Use ImageJ to crop and overlay images as well as measure pixel intensity. Create intensity plots using GraphPad PRISM software.

4 Notes

1. In case worms have to be moved to new *RNAi* plates in order to reach day 1 without being starved, prepare fresh overnight cultures every second day, follow the rest of the procedure, and transfer. Maintain streaking plates for up to 1 week.
2. In case worms have to be moved to new treatment plates in order to reach day 1 without being starved, prepare fresh etoposide or mitomycin C plates the same day and transfer.

3. If not all the quantity of the agarose solution is going to be used at once, aliquot the agarose solution in 1.5 mL tubes and store them at 4 °C for a week. Resolve at 100 °C in a water bath when needed and follow the protocol. Do not vortex or mix vigorously. Bubbles remain in the agarose solution for long and form gaps in the agarose pad.
4. In order to avoid dehydration of the agarose layer, which could interfere with the physiology of the worms before microscopy, we always use the agarose pads 10 min to 8 h after preparation.
5. Since in this protocol GFP::LGG-1 imaging is taking place, use only NaN_3 as an anesthetic. Levamisole may cause nonphysiological punctate structures [51].

Acknowledgments

We thank the *Caenorhabditis* Genetics Center (https://cgc.umn.edu/) and Daniel A. Starr for providing the DA2123 and UD626 strains, respectively. We thank Margarita-Elena Papandreou for generating the IR2969 strain. Work in the authors' laboratory is funded by the European Research Council under grant agreement "ERC-GA695190-MANNA," the European Union Horizon 2020 FETOPEN project "Dynamic," under the grant agreement "GA-863203," the Hellenic Foundation for Research and Innovation (H.F.R.I.) under the "1st Call for H.F.R.I. Research Projects to support Faculty members and Researchers and the procurement of high-cost research equipment" (Project Number: HFRI—FM17C3-0869, NeuroMitophagy), and the General Secretariat for Research and Innovation of the Greek Ministry of Development and Investments.

References

1. Jahed Z et al (2021) Molecular models of LINC complex assembly at the nuclear envelope. J Cell Sci 134(12)
2. Turkmen AM, Saik NO, Ullman KS (2023) The dynamic nuclear envelope: resilience in health and dysfunction in disease. Curr Opin Cell Biol 85:102230
3. Bone CR, Starr DA (2016) Nuclear migration events throughout development. J Cell Sci 129(10):1951–1961
4. Horvitz HR, Sulston JE (1980) Isolation and genetic characterization of cell-lineage mutants of the nematode Caenorhabditis elegans. Genetics 96(2):435–454
5. Sulston JE, Horvitz HR (1977) Post-embryonic cell lineages of the nematode, Caenorhabditis elegans. Dev Biol 56(1):110–156
6. Sulston JE, Horvitz HR (1981) Abnormal cell lineages in mutants of the nematode Caenorhabditis elegans. Dev Biol 82(1):41–55
7. Sulston JE et al (1983) The embryonic cell lineage of the nematode Caenorhabditis elegans. Dev Biol 100(1):64–119
8. Hedgecock EM, Thomson JN (1982) A gene required for nuclear and mitochondrial attachment in the nematode Caenorhabditis elegans. Cell 30(1):321–330
9. Malone CJ et al (1999) UNC-84 localizes to the nuclear envelope and is required for nuclear migration and anchoring during C. Elegans

development. Development 126(14): 3171–3181
10. Starr DA, Han M (2002) Role of ANC-1 in tethering nuclei to the actin cytoskeleton. Science 298(5592):406–409
11. Hao H et al (2021) The Nesprin-1/−2 ortholog ANC-1 regulates organelle positioning in C. Elegans independently from its KASH or actin-binding domains. elife 10
12. Gros-Louis F et al (2007) Mutations in SYNE1 lead to a newly discovered form of autosomal recessive cerebellar ataxia. Nat Genet 39(1): 80–85
13. Izumi Y et al (2013) Cerebellar ataxia with SYNE1 mutation accompanying motor neuron disease. Neurology 80(6):600–601
14. Dupre N et al (2007) Clinical and genetic study of autosomal recessive cerebellar ataxia type 1. Ann Neurol 62(1):93–98
15. Noreau A et al (2013) SYNE1 mutations in autosomal recessive cerebellar ataxia. JAMA Neurol 70(10):1296–1231
16. Razafsky D, Hodzic D (2015) A variant of Nesprin1 giant devoid of KASH domain underlies the molecular etiology of autosomal recessive cerebellar ataxia type I. Neurobiol Dis 78:57–67
17. O'Roak BJ et al (2011) Exome sequencing in sporadic autism spectrum disorders identifies severe de novo mutations. Nat Genet 43(6): 585–589
18. Yu TW et al (2013) Using whole-exome sequencing to identify inherited causes of autism. Neuron 77(2):259–273
19. Psychiatric GWAS Consortium Bipolar Disorder Working Group (2011) Large-scale genome-wide association analysis of bipolar disorder identifies a new susceptibility locus near ODZ4. Nat Genet 43(10):977–983
20. Green EK et al (2013) Association at SYNE1 in both bipolar disorder and recurrent major depression. Mol Psychiatry 18(5):614–617
21. Zhang Q et al (2007) Nesprin-1 and -2 are involved in the pathogenesis of Emery Dreifuss muscular dystrophy and are critical for nuclear envelope integrity. Hum Mol Genet 16(23): 2816–2833
22. Puckelwartz MJ et al (2009) Disruption of nesprin-1 produces an Emery Dreifuss muscular dystrophy-like phenotype in mice. Hum Mol Genet 18(4):607–620
23. Puckelwartz MJ et al (2010) Nesprin-1 mutations in human and murine cardiomyopathy. J Mol Cell Cardiol 48(4):600–608
24. Attali R et al (2009) Mutation of SYNE-1, encoding an essential component of the nuclear lamina, is responsible for autosomal recessive arthrogryposis. Hum Mol Genet 18(18):3462–3469
25. Sjoblom T et al (2006) The consensus coding sequences of human breast and colorectal cancers. Science 314(5797):268–274
26. Marme A et al (2008) Loss of Drop1 expression already at early tumor stages in a wide range of human carcinomas. Int J Cancer 123(9):2048–2056
27. Tessema M et al (2008) Promoter methylation of genes in and around the candidate lung cancer susceptibility locus 6q23-25. Cancer Res 68(6):1707–1714
28. Doherty JA et al (2010) ESR1/SYNE1 polymorphism and invasive epithelial ovarian cancer risk: an ovarian cancer association consortium study. Cancer Epidemiol Biomarkers Prev 19(1):245–250
29. Stransky N et al (2011) The mutational landscape of head and neck squamous cell carcinoma. Science 333(6046):1157–1160
30. Shah SP et al (2012) The clonal and mutational evolution spectrum of primary triple-negative breast cancers. Nature 486(7403):395–399
31. Schoppmann SF et al (2013) Novel clinically relevant genes in gastrointestinal stromal tumors identified by exome sequencing. Clin Cancer Res 19(19):5329–5339
32. Matsumoto A et al (2015) Global loss of a nuclear lamina component, lamin A/C, and LINC complex components SUN1, SUN2, and nesprin-2 in breast cancer. Cancer Med 4(10):1547–1557
33. Horn HF et al (2013) The LINC complex is essential for hearing. J Clin Invest 123(2): 740–750
34. Ungricht R, Kutay U (2017) Mechanisms and functions of nuclear envelope remodelling. Nat Rev Mol Cell Biol 18(4):229–245
35. Konstantinidis G, Tavernarakis N (2021) Autophagy of the nucleus in health and disease. Front Cell Dev Biol 9:814955
36. Park YE et al (2009) Autophagic degradation of nuclear components in mammalian cells. Autophagy 5(6):795–804
37. Rello-Varona S et al (2012) Autophagic removal of micronuclei. Cell Cycle 11(1): 170–176
38. Ivanov A et al (2013) Lysosome-mediated processing of chromatin in senescence. J Cell Biol 202(1):129–143
39. Changou CA et al (2014) Arginine starvation-associated atypical cellular death involves mitochondrial dysfunction, nuclear DNA leakage,

and chromatin autophagy. Proc Natl Acad Sci USA 111(39):14147–14152

40. Lan YY et al (2014) Dnase2a deficiency uncovers lysosomal clearance of damaged nuclear DNA via autophagy. Cell Rep 9(1): 180–192
41. Dou Z et al (2015) Autophagy mediates degradation of nuclear lamina. Nature 527(7576): 105–109
42. Akinduro O et al (2016) Constitutive autophagy and Nucleophagy during epidermal differentiation. J Invest Dermatol 136(7): 1460–1470
43. Baron O et al (2017) Stall in canonical autophagy-lysosome pathways prompts Nucleophagy-based nuclear breakdown in neurodegeneration. Curr Biol 27(23): 3626–3642 e6
44. Lu X, Djabali K (2018) Autophagic removal of farnesylated carboxy-terminal lamin peptides. Cells 7(4)
45. Li Y et al (2019) Nuclear accumulation of UBC9 contributes to SUMOylation of lamin A/C and nucleophagy in response to DNA damage. J Exp Clin Cancer Res 38(1):67
46. Papandreou M-E, Konstantinidis G, Tavernarakis N (2023) Nucleophagy delays aging and preserves germline immortality. Nat Aging 3(1):34–46
47. Klionsky DJ et al (2021) Guidelines for the use and interpretation of assays for monitoring autophagy (4th edition)(1). Autophagy 17(1): 1–382
48. Mochida K et al (2015) Receptor-mediated selective autophagy degrades the endoplasmic reticulum and the nucleus. Nature 522(7556): 359–362
49. Mochida K et al (2022) Atg39 links and deforms the outer and inner nuclear membranes in selective autophagy of the nucleus. J Cell Biol 221(2)
50. Zou CX et al (2023) The ortholog of human REEP1-4 is required for autophagosomal enclosure of ER-phagy/nucleophagy cargos in fission yeast. PLoS Biol 21(11):e3002372
51. Zhang H et al (2015) Guidelines for monitoring autophagy in Caenorhabditis elegans. Autophagy 11(1):9–27